

Host galaxy properties of mergers of stellar binary black holes and their implications for advanced LIGO gravitational wave sources

Liang Cao,^{1,2} Youjun Lu,^{1,2*} and Yuetong Zhao^{1,2}

¹National Astronomical Observatories, Chinese Academy of Sciences, 20A Datun Road, Beijing 100012, China

²School of Astronomy and Space Sciences, University of Chinese Academy of Sciences, 19A Yuquan Road, Beijing 100049, China

Accepted 2017 November 24; Received 2017 November 23; in original form 2017 October 9

ABSTRACT

Understanding the host galaxy properties of stellar binary black hole (SBBH) mergers is important for revealing the origin of the SBBH gravitational-wave sources detected by advanced LIGO and helpful for identifying their electromagnetic counterparts. Here we present a comprehensive analysis of the host galaxy properties of SBBHs by implementing semi-analytical recipes for SBBH formation and merger into cosmological galaxy formation model. If the time delay between SBBH formation and merger ranges from \lesssim Gyr to the Hubble time, SBBH mergers at redshift $z \lesssim 0.3$ occur preferentially in big galaxies with stellar mass $M_* \gtrsim 2 \times 10^{10} M_\odot$ and metallicities Z peaking at $\sim 0.6Z_\odot$. However, the host galaxy stellar mass distribution of heavy SBBH mergers ($M_{\bullet\bullet} \gtrsim 50 M_\odot$) is bimodal with one peak at $\sim 10^9 M_\odot$ and the other peak at $\sim 2 \times 10^{10} M_\odot$. The contribution fraction from host galaxies with $Z \lesssim 0.2Z_\odot$ to heavy mergers is much larger than that to less heavy mergers. If SBBHs were formed in the early universe (e.g., $z > 6$), their mergers detected at $z \lesssim 0.3$ occur preferentially in even more massive galaxies with $M_* > 3 \times 10^{10} M_\odot$ and in galaxies with metallicities mostly $\gtrsim 0.2Z_\odot$ and peaking at $Z \sim 0.6Z_\odot$, due to later cosmic assembly and enrichment of their host galaxies. SBBH mergers at $z \lesssim 0.3$ mainly occur in spiral galaxies, but the fraction of SBBH mergers occur in elliptical galaxies can be significant if those SBBHs were formed in the early universe; and about two thirds of those mergers occur in the central galaxies of dark matter halos. We also present results on the host galaxy properties of SBBH mergers at higher redshift.

Key words: stars: black holes – gravitational waves – black hole physics – galaxies: abundance – galaxies: statistics

1 INTRODUCTION

Gravitational wave (GW) events from mergers of stellar binary black holes (SBBHs) are now expected to be regularly detected by the advanced Laser Interferometer Gravitational Observatory (aLIGO), examples include GW150914 (Abbott et al. 2016a), GW151226 (Abbott et al. 2016b), GW170104 (Abbott et al. 2017a), and GW170814 (Abbott et al. 2017b). These detections not only confirm the existence of GWs and demonstrate the existence of SBBHs in the universe, but also offer a great tool to study the astrophysical origin of SBBHs and the abundant stellar and dynamical physics involved in, which are still not well understood, yet.

A number of mechanisms have been proposed to produce SBBH GW sources (e.g., Belczynski et al. 2002; Rodriguez et al. 2015, 2016; Mapelli 2016; Wang et al. 2016a; Sasaki et al. 2016; Wang et al. 2016b; McKernan et al. 2017), among which the evolution of massive binary stars in galactic fields in isolation is possibly the leading mechanism (e.g., Mandel & de Mink 2016; Belczynski et al. 2016b). According to comprehensive population synthesis modeling of the formation of SBBHs from binary zero-age main-sequence (ZAMS) stars (Belczynski et al. 2016b, for other SBBH population synthesis model, see also Portegies Zwart & Verbunt 1996; Spera et al. 2015; Spera & Mapelli 2017; Hurley et al. 2000, 2002), GW150914-like sources, i.e., mergers of heavy SBBHs, are required to be formed in metal poor environments (with metallicity $Z \lesssim 0.1Z_\odot$) at either

* E-mail: luyj@nao.cas.cn

an early time of the universe (with a corresponding redshift of $z \gtrsim 3$) or very recently ($z \sim 0.2$) (see also Abbott et al. 2016a; Hartwig et al. 2016; Lamberts et al. 2016; O’Shaughnessy et al. 2017; Elbert et al. 2017; Schneider et al. 2017). If this is true, then the host galaxies of those GW150914-like sources at the GW detection time may be either massive or small (e.g., O’Shaughnessy et al. 2010; Lamberts et al. 2016; O’Shaughnessy et al. 2017; Elbert et al. 2017; Schneider et al. 2017). It is anticipated that the properties of the host galaxies of GW sources, if identified by future observations, can be used to reveal the formation mechanism for SBBHs and constrain the physics involved in the SBBH formation processes.

To identify the origin of GW sources, one of the crucial ways is to find their electro-magnetic (EM) counterparts, if any, since the localization of these sources, obtained from GW signals only, is poor (typically covering a sky area of hundreds of square degrees with more than ten thousands of galaxies in it) (Abbott et al. 2016c). Great efforts have been put into searching for EM counterparts of GW sources via broadband campaign (e.g., GW150914). After the submission of this paper, GW signals emitted from a binary neutron star merger (GW170817) have been detected by aLIGO and Virgo with greatly improved localization (Abbott et al. (2017c)), and its EM counterpart, a short gamma ray burst (GRB170817A) and kilonova, is found by subsequent multiband observations (Abbott et al. (e.g., 2017d)). However there still seems little expectation of the detection of EM counterparts for SBBH mergers (Abbott et al. 2016d). If the host galaxy properties of GW sources can be known, the search for EM counterparts would be greatly narrowed. Therefore, it is of great importance to figure out where and when the GW sources were formed and what kind of galaxies they are hosted in at the GW detection time by the means of searching for the EM counterparts of SBBH GW sources.

Some attempts have been made on investigating the host galaxies of SBBH GW sources (e.g., Lamberts et al. 2016; O’Shaughnessy et al. 2017; Elbert et al. 2017; Schneider et al. 2017) since the discovery of GW150914. By combining observational estimates of galaxy properties across cosmic time and considering the effects of galaxy mergers, Lamberts et al. (2016) found that the GW150914-like sources may be dominated by binaries in massive galaxies formed at early time (with $z \simeq 2$) if their progenitors have metallicity $Z \geq 0.1Z_{\odot}$ while come from binaries in dwarf galaxies formed at later time (with $z \simeq 0.5$) if $Z < 0.1Z_{\odot}$, which appears somewhat different from Belczynski et al. (2016a). Using detailed cosmological simulations of Milky way-like halos, Schneider et al. (2017) found that GW150914-like sources may be formed in low-metallicity dwarf galaxies at high redshift ($2.4 \leq z \leq 4.2$) but be mostly hosted by star forming galaxies with mass $> 10^{10} M_{\odot}$. Elbert et al. (2017) also investigated the host galaxy properties of GW sources by using the observed properties of galaxies and found that SBBH mergers would be mostly localized in dwarf galaxies if the merger timescale is short but in massive galaxies otherwise. Difference among the results output from the above different approaches may be due to the use of different input models for the BH-BH properties, the limitations (or uncertainties) in using scaling relations and its extrapolations, or lack of in-

formation on SBBHs formed in each galaxy (see discussions in Schneider et al. 2017). Although Schneider et al. (2017) did consider the SBBH formation history in individual galaxies by using cosmological simulations but it is limited to a small volume (size of 4 cMpc) and halos with mass up to Milky way-size. Mapelli et al. (2017) recently considered the SBBH formation by using the Illustris simulation of galaxy formation in a large box (106.5 Mpc), but focused on the the merger rate density evolution and the effect of metallicity.

In this paper, we investigate the properties of the host galaxies of the SBBH GW sources by implementing simple SBBH formation recipes into a cosmological galaxy formation model. In this approach, the cosmological N-body Millennium-II simulation in a box of side 137 Mpc (Boylan-Kolchin et al. 2009), semi-analytical galaxy formation recipes (Guo et al. 2011), and simple recipes for SBBH formation following the star formation in each galaxy are combined together. Therefore, the SBBH formation histories in a large number of individual galaxies with masses from $10^7 M_{\odot}$ to several times of $10^{11} M_{\odot}$ are also resolved. In section 2, we describe the model for SBBH formation and SBBH mergers by utilizing the cosmological galaxy formation model results presented in Guo et al. (2011) and simple recipes for SBBH formation from the evolution of binary stars and SBBH mergers since then in each individual model galaxies. We generate mock catalogs for SBBHs, SBBH mergers, and their host galaxies in section 3. According to the mock samples, statistics on the properties of the host galaxies of SBBH GW sources are obtained and presented in section 4. Conclusions and discussions are given in section 5.

2 BINARY BLACK HOLES FORMATION AND MERGER SCENARIO

In general, the birth rate R_{birth} of single BHs with mass m_{\bullet} per unit volume per unit time at the cosmic time t can be estimated by (see also Abbott et al. 2016f; Dvorkin et al. 2016),

$$R_{\text{birth}}(m_{\bullet}, t) = \int \int \psi[Z; t - \tau(m_{\star})] \phi(m_{\star}) \times \delta(m_{\star} - g_{\bullet}^{-1}(m_{\bullet}, Z)) dm_{\star} dZ. \quad (1)$$

Here $\psi(Z; t)$ is the star formation rate with metallicity Z per unit volume per unit time at the cosmic time t , $\tau(m_{\star})$ is the lifetime of a star with mass m_{\star} , $\phi(m_{\star}) \propto m_{\star}^{-\alpha}$ is the initial mass function (IMF) and the Chabrier IMF (Chabrier 2003) is adopted below,¹ δ is the Dirac- δ function, $m_{\bullet} = g_{\bullet}(m_{\star}, Z)$ is a function that describes the relation between the mass of a stellar remnant BH and the mass of its progenitor star and the latest version given in Spera et al. (2015) is adopted in this paper. Note that the results on the relation between remnant BH mass and progenitor mass obtained by Woosley & Weaver (1995) and Fryer et al. (2012) are also frequently adopted in the literature, but alternatively adopting those results does not lead to significant effects on our

¹ Note here that the dependence of the black hole formation on the assumed IMF is weak (Elbert et al. 2017).

conclusions (see also discussions in [Elbert et al. 2017](#)). Since the evolution time of BH progenitors are just a few times 10^6 yr, which is negligible compared with the evolution time of galaxies, therefore, we ignore $\tau(m_*)$ in the following calculations.

Considering SBBHs formed from isolated massive binary stars in galactic fields, only a fraction ($f_{b,*}$) of stars are in binaries, a fraction ($f_{\bullet\bullet}$) of binary that can evolve to SBBHs, a fraction (f_q) of SBBHs that have large mass ratio $q = m_{\bullet,2}/m_{\bullet,1}$ with $m_{\bullet,1}$ and $m_{\bullet,2}$ the masses of the primary component and the secondary one, respectively, and a fraction (f_{mrg}) of them that can merger within the Hubble time. An SBBH may merger after a time period of t_d since its formation due to its orbit decay by GW radiation. The GW event rate is then given by the convolution of the birthrate $R_{\text{birth}}(m_{\bullet,1}, q; t)$ with the delay time distribution $P(t_d)$ (see a similar approach by [Dvorkin et al. \(2016\)](#)), i.e.,

$$R_{\text{GW}}(m_{\bullet,1}, q; t) = f_{\text{eff}} \int_{t_1}^{t_u} R_{\text{birth}}(m_{\bullet,1}, t-t_d) P_q(q) P_t(t_d) dt_d, \quad (2)$$

and

$$f_{\text{eff}} = f_{b,*} \times f_q \times f_{\bullet\bullet} \times f_{\text{mrg}}. \quad (3)$$

Here the distribution of mass ratio $P_q(q)$ is assumed to be independent of the BH mass and is normalized as $\int_{q_{\text{min}}}^1 P_q(q) dq = 1$, f_{eff} is the effective factor to form GW sources from binary stars, $t_1 = t_{d,\text{min}}$ is the minimum time delay, $t_u = \int_{z(t)}^{\infty} \left| \frac{dt}{dz} \right| dz$ is the longest possible time delay for an SBBH merger occurred at the cosmic time t and correspondingly redshift z .

As seen from equations (1) and (2), the event rate of SBBH GW sources depends on not only the (binary) star formation rate, but also the mass ratio distribution $P_q(q)$ and the distribution of the delay time $P_t(t_d)$ between the binary formation and the final merger. Distributions P_q and P_t depend on detailed physics involved in the evolution processes of massive binary stars towards SBBHs and are expected to not directly depend on their environment at large scales, e.g., host galaxies (see sections 2.2 and 2.3). The star formation rate $\psi(Z; t)$ is the cosmic mean star formation rate averaged over all galaxies, which can be obtained from observations (e.g., as that adopted in [Dvorkin et al. 2016](#)). Considering that the star formation histories of different GW host galaxies can be significantly different, therefore, equation (1) can be replaced by

$$\begin{aligned} R_{\text{birth}}(m_{\bullet}, t) &= \frac{1}{\Delta V \delta t} \sum_{i=1}^N \mathcal{R}_{\text{birth},i}(m_{\bullet}, t), \quad (4) \\ \mathcal{R}_{\text{birth},i}(m_{\bullet}, t) &= \int \int \sum_j \Psi_{ij}[Z_{ij}; t - \tau(m_*)] \phi(m_*) \times \\ &\quad \delta(m_* - g_{\bullet}^{-1}(m_{\bullet}, Z_{ij})) dm_* dZ_{ij}. \quad (5) \end{aligned}$$

Here ΔV is the comoving volume of the observable universe or a comoving volume that is considered (e.g., a simulation box) at the cosmic time from t to $t + \delta t$, $\mathcal{R}_{\text{birth},i}$ is the total number of single BHs with mass $m_{\bullet} \rightarrow m_{\bullet} + dm_{\bullet}$ over a time period of $t \rightarrow t + \delta t$ in a galaxy i or its progenitors (t is a time earlier than the detection time of the galaxy i), $i = 1, \dots, N$ indicate all galaxies in the volume ΔV , Ψ_{ij} represents the total mass of stars formed in galaxy j in the time period

$t \rightarrow t + \delta t$, one of the progenitor galaxies of galaxy i , Z_{ij} is the metallicity of the star forming gas in the progenitor galaxy j , and the summation is for all progenitor galaxies of the galaxy i . The GW event rate of a single galaxy i at the cosmic time t is given by

$$\mathcal{R}_{\text{GW},i}(m_{\bullet,1}, q; t) \propto \int_{t_1}^{t_u} R_{\text{birth},i}(m_{\bullet,1}, t-t_d) P_q(q) P_t(t_d) dt_d, \quad (6)$$

and the mean GW event rate per unit volume per unit time is given by the summation of the contribution from all galaxies

$$R_{\text{GW}}(m_{\bullet,1}, q; t) = f_{\text{eff}} \sum_{i=1}^N \mathcal{R}_{\text{GW},i}(m_{\bullet,1}, q; t). \quad (7)$$

2.1 $\Psi_{ij}(Z_{ij}; t)$ for individual mock galaxies from a cosmological galaxy formation model

In order to study the host galaxy properties of those GW events, we use the catalogs of mock galaxies obtained from semi-analytical galaxy modeling by [Guo et al. \(2011\)](#), in which the assembly and star formation histories of each individual mock galaxy and its progenitors are given. These catalogs are obtained from the halo/subhalo merger trees of the Millennium II simulation ([Boylan-Kolchin et al. 2009](#)) by implementing parameterized semi-analytical modeling of the galaxy formation recipes of a variety of physics processes, e.g. a mass-dependent model for supernova feedback, more realistic treatments of gaseous and stellar disk growth, a updated reionization model. The free parameters of these models are determined by using the observed abundance, structure and clustering of low redshift galaxies as a function of stellar mass ([Guo et al. 2011](#)).

The outcome of the catalog is stored in a box with comoving size of 137 Mpc for 68 snapshots with redshift from 127.0 to 0. For each individual galaxy in each snapshot, its properties, such as position, stellar mass (M_*, Z_*), star formation rate ($\Psi_{ij}/\delta t$), star forming gas metallicity (Z_{ij}), and its identity ID (described by i, j, t) in the merger tree, are all recorded. Therefore, how many SBBH mergers or GW events happened in the time period $t \rightarrow t + \delta t$ in a galaxy can be obtained from the amount of stars formed at the time $t - t_d$ in the progenitor(s) of that galaxy according to equation (5).

2.2 $P_t(t_d)$

A significant fraction of SBBHs that merge at low redshift may have actually formed in the early universe, therefore GW events can be used to investigate the formation of BHs and SBBHs at a much earlier time (see eq. 2), which are otherwise invisible to current electromagnetic observations. The dependence of SBBH GW events on the the star formation history is significantly affected by the accuracy of the estimate of $P_t(t_d)$, which appears not well understood because of various uncertainties in the binary evolution model.

In most cases, t_d can be comparable to the age of the Universe, and it generally depends on the initial orbital configuration of binaries. Theoretical studies have shown that $P_t(t_d) \propto t_d^{-1}$ (e.g., [O'Shaughnessy et al. 2008, 2010](#);

Belczynski et al. 2016b; Lamberts et al. 2016). The minimum time delay is on the order of \lesssim Gyr but with some uncertainties. In this paper, we adopt two values for the minimum time delay $t_{d,\min}$, i.e., 50 Myr and 2 Gyr. We denote the first one as the “reference model” and the second one as the “large time delay model”. We also adopt two extreme models for $P_t(t_d)$, one is the prompt model with $P_t(t_d) \propto \delta(t_d)$, i.e., SBBHs merge right after their formation; the other one is a model for early formation of SBBHs at redshift $z > 6$ (denoted as the “early formation model”), for which $P_t(t_d) \propto 1/t_d$, $t_{d,\min} = \max[t(z) - t(z = 6), 50 \text{ Myr}]$, and $t(z) = \int_z^\infty \left| \frac{dt}{dz'} \right| dz'$ is the cosmic age at redshift z . The prompt model introduced in this paper is only for the comparison with other models. Assuming the prompt model, the GW event rate should be roughly determined by the number of stars formed at the GW detection time. In other three models, the GW event rate is determined by the number of all stars formed earlier than the time that is about $t_{d,\min}$ before the GW detection time.

The set of the “early SBBH formation model” is based on that the detected heavy SBBHs, i.e., GW150914, GW170104, and GW 170814, may have to be formed from metal poor massive binary stars at high redshift ($z \gtrsim 3$; e.g., Abbott et al. 2016f; Belczynski et al. 2016b; Hartwig et al. 2016). It is also anticipated that a significant fraction of the future aLIGO SBBH detections might be originated from those metal poor massive binary stars formed at very high redshift, possibly Pop III stars, and these SBBHs are probably hosted in highly biased systems.

2.3 $P_q(q)$

According to population synthesis models, SBBH mergers resulting from evolution of massive binary stars typically have comparable mass components and $P_q(q)$ peaks at 0.8 – 1.0 (e.g., de Mink et al. 2013; Belczynski et al. 2016a,b). The formation of low mass ratio SBBHs is suppressed because low mass ratio binary stars, with sufficiently small separations, tend to merge with each other before they can evolve to SBBHs. Moreover, the mass ratio extends to lower values with decreasing total mass of SBBHs. In principle, reliable estimates of $P_q(q)$ may be obtained by intensive population synthesis model calculations, which can be included in equation (2) to generate SBBHs. However, we note here that the difference in $P_q(q)$ for SBBHs with different total mass seems not very significant (see Belczynski et al. 2016b), therefore, we assume $P_q(q) \propto q$ over the range from 0.5 to 1, which seems to be consistent with population synthesis results and compatible with the current aLIGO detections (e.g., Abbott et al. 2016a,b, 2017a). We note here that this setting does not affect our results on the host galaxy properties since the mass ratio of SBBHs formed from massive binary stars in galactic fields is independent of their environment at large scale.

With the above prescription, we can estimate the GW event rate of SBBH mergers according to equations (5)-(7) by using the catalog of mock galaxies with detailed assembly histories given by Guo et al. (2011). For comparison, we can also estimate the GW event rate of SBBH mergers by using observationally determined SFR and mean metallicity evolution according to equation (2). To do this calculation, we adopt the extinction-corrected SFR obtained by

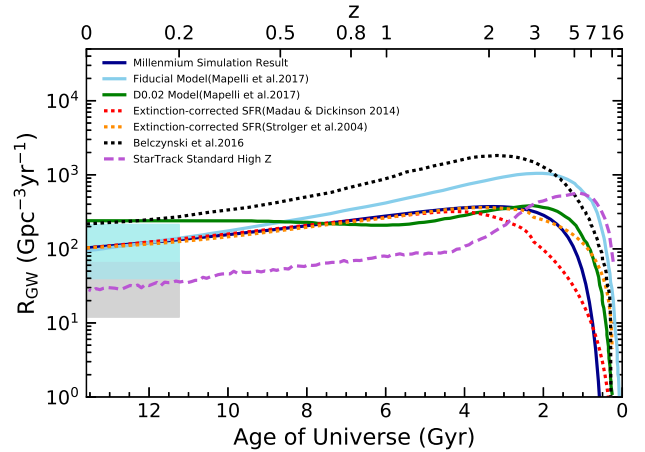


Figure 1. SBBH merger rate density as a function of the age of universe or redshift z . The blue solid line represents the results obtained from the Millennium simulation galaxy catalog assuming the reference model for the time delay. The red and orange dotted lines represent our model results by using the extinction-corrected specific star formation rate given by Madau & Dickinson (2014) and Strolger et al. (2004), respectively, and the mean metallicity redshift evolution in Belczynski et al. (2016a). The black dotted line represents the result obtained by Belczynski et al. (2016a) by using the extinction-corrected specific star formation rate in Madau & Dickinson (2014) and the binary population synthesis code StarTrack. The green and light blue solid lines represent respectively the results from the fiducial model and the D0.02 model in Mapelli et al. (2017) by planting BBHs obtained from the binary population synthesis code SEVN into the Illustris simulations. The purple dashed line represents the merger rate density obtained by Dominik et al. (2013). The cyan and grey shaded regions represent the constraints on the merger rate density obtained from those detected GW sources by assuming two different IMF, respectively (Abbott et al. 2017a).

Madau & Dickinson (2014, see their Eq. 15) and also the one obtained by Strolger et al. (2004, See their Eq. 5), and we adopt the mean metallicity redshift evolution as that in Belczynski et al. (2016a).

Note that in the above approach all the physics governing the evolution of SBBHs are encoded in the three independent functions f_{eff} , $P_q(q)$ and $P_t(t_d)$, and any correlation between the mass distribution of SBBHs and their merger times is ignored although there should be such a correlation as a result of the selected evolutionary pathways followed by massive BBHs systems. However, there are still large uncertainties in the evolution models of massive (binary) stars, especially, the large uncertainties in the understanding of a number of physical processes, such as the common envelope evolution, the kick from supernova explosion, and the mass transfer etc. (e.g., Dominik et al. 2013; Mapelli et al. 2017; Dvorkin et al. 2017). Different models may result in significantly different merger rate densities. Below we show that our simple approach can give similar merger rate density evolution compared against those obtained by using binary population synthesis codes.

Current detections of GW150914, GW151226, and GW170104 have already put a constraints on the merger

rate of SBBHs in the local universe as $40 - 213$ or $12 - 65 \text{ Gpc}^{-3} \text{ yr}^{-1}$ if assuming a Salpeter IMF or uniform in log-distribution for the primary components of progenitor binary stars (Abbott et al. 2017a, see the cyan- and grey-shaded regions in Fig. 1). We adopt that constraint on the mean detection rate of $103 \text{ Gpc}^{-3} \text{ yr}^{-1}$ to calibrate the merger rate density obtained from different models and thus constrain the unknown value f_{eff} . We find that f_{eff} should be $\sim 8.0 \times 10^{-4}$, $\sim 1.1 \times 10^{-3}$, $\sim 9.9 \times 10^{-2}$, and $\sim 1.2 \times 10^{-3}$, for the reference model, the large time delay model, the early SBBH formation model, and the prompt model, respectively. The value on f_{eff} for the reference model is roughly consistent with that obtained in Elbert et al. (2017). We note here that the distributions of the host galaxy properties of SBBH mergers obtained in this paper for each model are not affected by the actual value of f_{eff} .

Figure 1 shows the results on the merger rate density distribution as a function of redshift by adopting the reference model for $P_t(t_d)$. As seen from this figure, the merger rate density obtained by using the mock galaxy catalog from Guo et al. (2011) (blue line) is consistent with that obtained by using the observationally determined SFR from Strolger et al. (2004) (yellow dotted line) or from Madau & Dickinson (2014) (red dotted line), especially at redshift $z \lesssim 2$. The substantial differences at higher redshift are mainly due to the differences in the SFRs.

For comparison, we also plot a number of estimates for the merger rate density evolution obtained in the literature by using the binary population synthesis model in Figure 1. These estimates include the one by Belczynski et al. (2016a) using the observationally determined SFR and the binary population synthesis code StarTrack (black dotted line), by Mapelli et al. (2017) using the SFR of individual galaxies resulting from the Illustris simulation and a new version of binary evolution code BSE (green and cyan lines representing two different models), by Dominik et al. (2013) using the StarTrack code and mock galaxies generated from Press-Schechter like formalism. The results obtained by using the binary population synthesis models can be substantially different depending on the settings of the model parameters describing supernova explosion, common envelope evolution, mass transfer, and the supernova kick, etc. It can be seen from Figure 1 that the shape of the merger rate density evolution resulting from our simple prescription is only slightly shallower than most of those obtained by using binary population synthesis model at least at redshift $z \lesssim 2$ but steeper than the D0.02 model in Mapelli et al. (2017). At higher redshift $z > 2 - 3$, our simple model results in comparable similar merger rate as the D0.02 model in Mapelli et al. (2017), but it results in relatively less SBBH mergers compared with others shown in Figure 1 obtained from the population synthesis models, which may be partly due to the ignorance of the correlation between the mass distribution of SBBHs and their merger times and the different SFR and metallicity distribution adopted in different models.

3 MOCK SAMPLES

Using the mock galaxy catalogs and the assembly and star formation history of each mock galaxy, we randomly assign SBBH merger GW events according to the probabil-

ity resulting from equation (6) for individual galaxies across cosmic time. We also impose that $\min[m_{\bullet,1}, m_{\bullet,2}] \geq 5M_{\odot}$, which is set by considering that all BHs measured dynamically have masses $\gtrsim 5M_{\odot}$ (e.g., Özel et al. 2010; Farr et al. 2011, for the evidence of a mass gap at $3 - 5M_{\odot}$). With these procedures, we can obtain mock catalogs of SBBH GW events at any given cosmic time t (or correspondingly redshift z) for given $P_t(t_d)$ and $P_q(q)$. We generate a number of mock catalogs of SBBH GW events at a number of redshifts (e.g., $z = 0.3, 1$, and 2 , respectively) that enables the statistic studies on the properties of their host galaxies. Each GW event is characterized by the masses of the two components, i.e., $m_{\bullet,1}$ and $m_{\bullet,2} = qm_{\bullet,1}$, the merger time $t(z)$, the SBBH formation time $t(z) - t_d$, the position and other properties (e.g., stellar mass M_* , metallicity Z_* , and morphology) of its host galaxy, and the total mass (M_{halo}) of their dark matter halo at the merger time $t(z)$, and the properties of its progenitor galaxy that the SBBHs formed in at the SBBH formation time $t - t_d$.

We note here that some of those mock SBBHs may have received considerable kicks due to supernovae explosions and moved away from their birth places. Mandel (2016) estimated the kicks according to available observations on the black hole X-ray binaries (BHXBs) and he found that the kick velocity is not required to be $> 80 \text{ km s}^{-1}$, although larger kicks are not completely ruled out, yet (see Repetto et al. 2012). Mirabel (2016) also suggests that the kick velocity should be small and insignificant according to the kinematics of BHXBs. If assuming a kick velocity of 80 km s^{-1} , most of the SBBHs would not be able to climb out from the potential of their host dark matter halos at the SBBH formation time, as the mass of the host dark matter halos at the SBBH formation time is typically larger than $10^{10} M_{\odot}$ with escape velocity $\gtrsim 100 \text{ km s}^{-1}$. Therefore, we ignore the possible offsets, if any, of the SBBH mergers at the GW detection time from those galaxies they formed in. However, we note that larger kick velocity is still possible, with which some BBHs may locate at the outskirts of or even climb out from the potential of their host galaxies and dark matter halos they formed in, especially when those hosts are small as Perna et al. (2017) recently investigated in.

4 MODEL RESULTS

4.1 Stellar mass distributions of SBBH host galaxies

We extract the statistical information on their host galaxies from the mock catalogs for SBBH GW events and SBBHs. Figure 2 shows the stellar mass distribution of the host galaxies of those SBBHs at their merger time (i.e., the GW detection time $z = 0.3, 1.0$, and 2.0 ; thick lines) and formation time (thin lines), respectively. For those GW events detected at low redshift (e.g., $z = 0.3$, top panel), the host stellar mass distribution at the SBBH formation time resulting from the reference model (or the large time delay model) peaks at $1.8 \times 10^{10} M_{\odot}$ (or $1.9 \times 10^{10} M_{\odot}$) with a 5 to 95 percentile range of 1.7×10^8 to $5.3 \times 10^{10} M_{\odot}$ (or 1.2×10^8 to $4.4 \times 10^{10} M_{\odot}$) (thin lines in the top panel), while at the SBBH merger time it peaks at $3.3 \times 10^{10} M_{\odot}$ (or $3.3 \times 10^{10} M_{\odot}$) with a 5 to 95 percentile range of 7.0×10^8

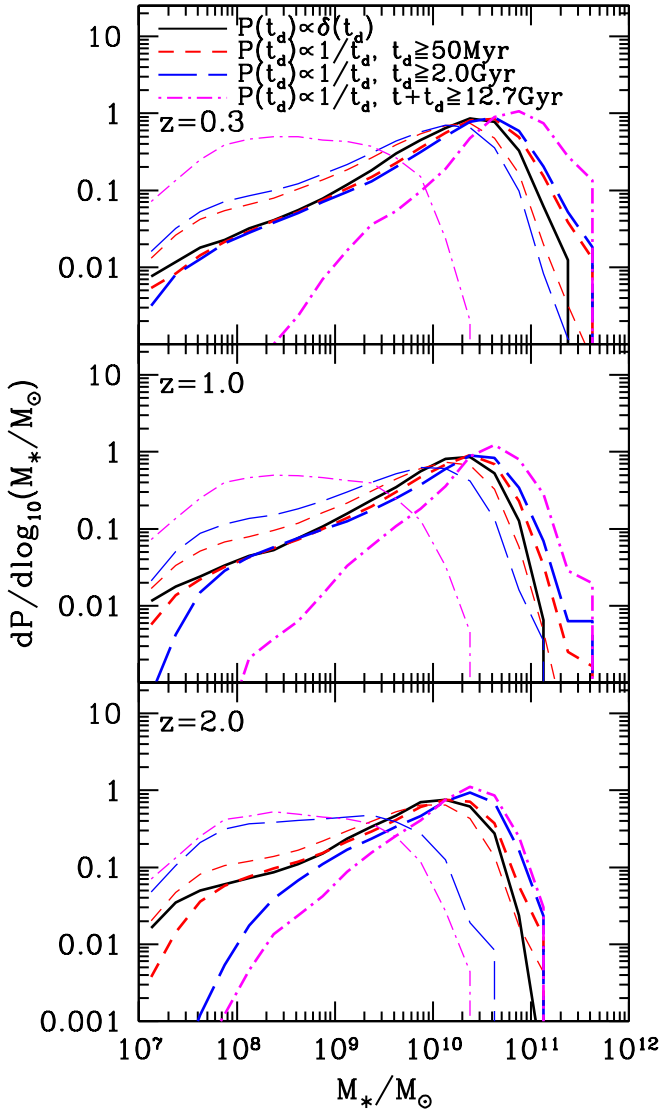


Figure 2. Stellar mass distribution of the host galaxies of binary black holes (SBBHs) at the SBBH formation time (thin lines) and merger time/GW detection time (thick lines). Top, middle and bottom panels show those distributions for SBBHs if the GW signals due to their mergers were detected at redshift $z = 0.3$, 1, and 2, respectively. In each panel, black solid line shows the results obtained from the prompt model in which two SBBH components merge with each other right after the SBBH formation. The red short-dashed, blue long-dashed, and magenta dot-dashed lines show the results obtained from those time delay models $P(t_d) \propto 1/t_d$ with $t_d \geq 50$ Myr, ≥ 2 Gyr, and ≥ 12.7 Gyr $- t(z)$, i.e., the reference model, the large time delay model, and the early SBBH formation model, respectively. Here $t(z) = \int_z^\infty \left| \frac{dt}{dz} \right| dz$ and 12.7 Gyr are the cosmic age at redshift z and at $z = 6$, respectively.

to $9.8 \times 10^{10} M_\odot$ (or 7.6×10^8 to $1.1 \times 10^{11} M_\odot$; thick line in the top panel). The distribution of the SBBH host galaxies at the GW detection time is shifted to significant higher masses compared with that at the SBBH formation time simply because of the growth of those host galaxies after the SBBH formation. For those GW events detected at higher redshifts

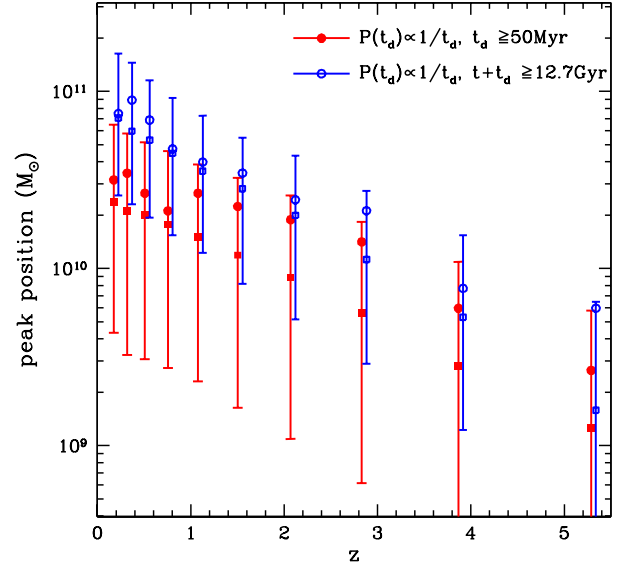


Figure 3. Peak and median positions of the probability distribution of the GW host galaxies as a function of merger redshift. The red solid circles and squares show the peaks and the medians for the reference model with $P(t_d) \propto 1/t_d$ and $t_{d,\min} \geq 50$ Myr, and the blue open circles and squares show the peaks and the medians for the early SBBH formation model with $P(t_d) \propto 1/t_d$ and $t_{d,\min} \geq 12.7$ Gyr $- t(z)$, respectively. Vertical bars indicate the probability range of 16% percentile to 84% percentile of host galaxies with mass from low to high. Note that a small horizontal offset is added to each point obtained from the early SBBH formation model, for clarity.

(e.g., $z = 1, 2$), similar trends are also seen, but both distributions at the SBBH formation time and the GW detection time are substantially decrease at the high mass end and the distribution peaks shift toward lower masses.

If the SBBHs were formed at early time, e.g., $z \gtrsim 6$ (magenta dot-dashed lines for the early SBBH formation model), their host galaxies are small at the SBBH formation time and the host stellar mass distribution peaks at $2.8 \times 10^8 M_\odot$ with a 5 to 95 percentile range of 2.2×10^7 to $3.5 \times 10^9 M_\odot$; while at the GW detection time, even at $z = 2$ (magenta dot-dashed lines in the bottom panel), their host galaxies grew significantly since their formation and become massive, and the host stellar mass distribution peaks at $2.2 \times 10^{10} M_\odot$; the SBBH host galaxies became even more massive if those SBBHs merged at $z = 0.3$ (magenta dot-dashed line shown in the top panel), and the host stellar mass distribution peaks at $7.5 \times 10^{10} M_\odot$ with a 5 to 95 percentile range of 7.5×10^9 to $2.1 \times 10^{11} M_\odot$. If SBBHs merger right after their formation, i.e., the prompt model, the host stellar mass distribution at the merger time is the same as that at the formation time. Assuming this model, if the SBBH mergers were detected at $z \sim 0.3$, their host galaxy mass distribution peaks at $\sim 2.0 \times 10^{10} M_\odot$ and the peak position shifts slightly towards lower masses with increasing detection redshift.

Figure 3 shows the peak and median of the host galaxy stellar mass distributions of SBBH mergers at different GW detection time. The red filled circles and blue open circles represent those resulting from the reference model and the early SBBH formation model, i.e., $P(t_d) \propto 1/t_d$ with

$t_d \geq 50$ Myr, and $t_d \geq 12.7$ Gyr $- t(z)$, respectively. The bars associated with each point mark the 16 and 84 percentile of the distribution from low to high mass, respectively. Apparently, the peak and median masses of those distributions resulting from the early SBBH formation model is substantially larger than those resulting from the reference model, especially at low redshift (e.g., $z < 1.5$). Furthermore more, the reference model results in a substantially wider range of the host stellar mass at the GW detection time compared with the early SBBH formation model. The reason is as follows. The host galaxies of those SBBH mergers in the early SBBH formation model were mainly formed from high density peaks in the early universe, which grew up and collapsed into more massive objects in their subsequent evolution. The later the SBBH mergers were detected, the more massive the SBBH host galaxies. However, the host galaxies of those SBBH mergers in the reference model may be formed from both high density peaks in the early universe and not so high density peaks at a time not long before the SBBH merger time. Therefore, the mass distribution resulting from the reference model covers a wider range compared to that from the early SBBH formation model, and the peak and median masses of the former one are also substantially smaller than those of the latter one, especially at low redshift, as shown in Figure 3. These results suggest that the mass distribution of the host galaxies of SBBH GW sources is sensitive to the delay times and formation redshifts of these systems.

4.2 Morphologies and types of SBBH host galaxies

The host galaxies of GW events may have different types. Some SBBH GW events may be hosted in elliptical galaxies and some others are hosted in spiral galaxies. Some SBBH GW events may occur in central galaxies or satellite galaxies in big halos, and some others may occur in isolated galaxies in small dark matter halos or satellites in sub-halos. Similar as that in Guo et al. (2011), elliptical and spiral are discriminated by using the bulge mass to total stellar mass ratio. A mock galaxy is labeled as an elliptical if its bulge mass to total stellar mass ratio is larger than 0.8, and otherwise it is labeled as a spiral. If a mock galaxy is in the main subhalo of their host dark matter halo, it is labeled as the central galaxy of that halo; if it is in other subhalos, it is labeled as a satellite; and if it is the only galaxy in the halo, it is labeled as an isolated galaxy.

The fraction of those GW events that are hosted in ellipticals or spirals depends on when and where those SBBHs were formed. Figure 4 shows the probability distribution of those GW host galaxies in different morphological types at the GW detection time $z = 0.3$ for different $P_t(t_d)$ models. As seen from this Figure, if the time period between the SBBH formation and merger distributed in a broad range from ~ 50 Myr to the Hubble time (the reference model), the host galaxies of SBBH mergers with $M_{\bullet\bullet} \geq 10M_{\odot}$ at $z = 0.3$ are mostly spiral galaxies with the 5% – 95% percentile stellar mass range of $\sim 5.3 \times 10^8 - 6.0 \times 10^{10} M_{\odot}$, and only about 13% are in elliptical galaxies. If those SBBHs were formed at early time (e.g., $z > 6$, the early SBBH formation model) and detected through GW at $z = 0.3$, about 47% of the GW events occur in elliptical galaxies with mass $\gtrsim 7.0 \times 10^9 M_{\odot}$ and others are in spiral galaxies typically

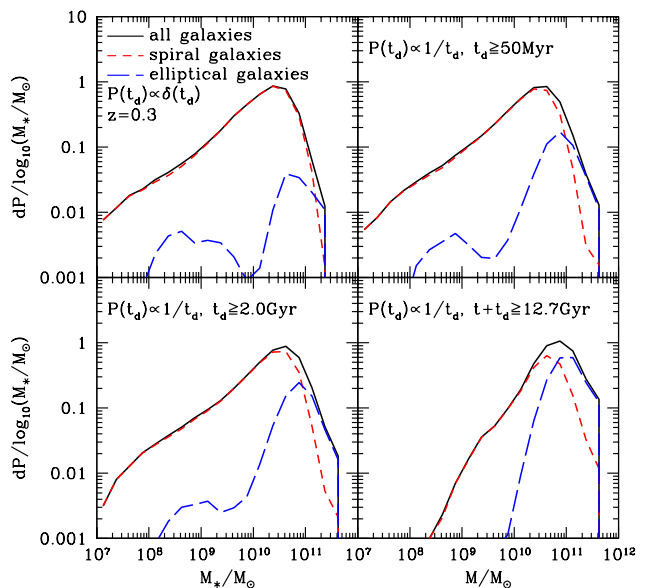


Figure 4. Distributions of the host galaxies of those SBBH mergers as a function of galaxy stellar mass for host galaxies with different morphologies, including ellipticals and spirals.

with mass $\sim 4.2 \times 10^9 - 9.4 \times 10^{10} M_{\odot}$; if SBBHs merge shortly after their formation (i.e., the prompt model), then $\sim 96\%$ of them should be hosted in spiral galaxies with mass $\sim 5.3 \times 10^8 - 5.3 \times 10^{10} M_{\odot}$ and no more than 4% are in elliptical galaxies (top left panel). Apparently, the longer the merger time, the larger the fraction of ellipticals in those SBBH host galaxies. The reason is as follows. Spiral galaxies formed at early time may merge into each other and form ellipticals in their later evolution. The longer the evolution time, the larger the probability for this morphology transformation. Therefore, the fraction of the SBBHs mergers hosted in ellipticals grows with time if most SBBHs were originally formed in spirals at early time.

Figure 5 shows the probability distribution of those SBBH GW events that are hosted in central galaxies, satellites, and isolated galaxies, separately. For four different $P_t(t_d)$ models (shown in the top-left, top-right, bottom-left, and bottom-right panels), the fraction that the SBBH GW events are hosted in central galaxies (or satellites) are 80% (or 19%), 66% (or 23%), 61% (or 25%), and 62% (or 22%), respectively. As seen from this Figure, most of the SBBH GW events are hosted in central galaxies. The reason is as follows. The contribution from central galaxies to the star formation rate is more significant compared with that from satellites and isolated galaxies. Therefore, more SBBHs were formed in central galaxies. After the SBBH formation, some of those central galaxies maintain as central galaxies of their growing host halos, some of them merger with other central galaxies or satellites to form new central galaxies, though a small fraction of those central galaxies do sink into big halos to become satellites. At the SBBH merger time, the host galaxies are still preferentially centrals, almost independent of the delay time model.

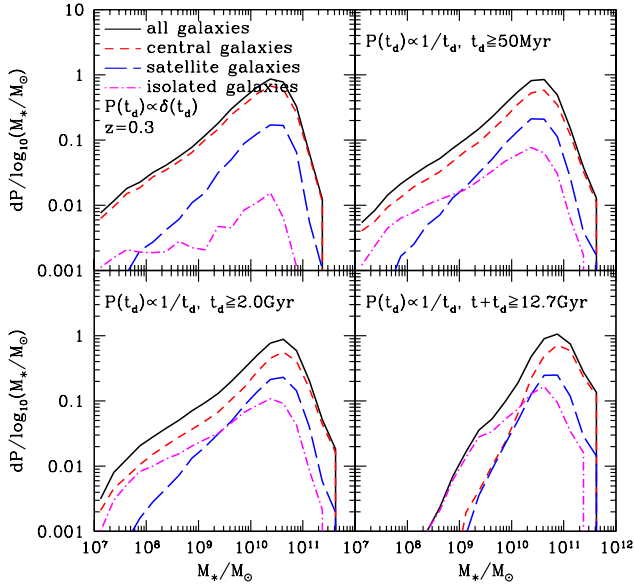


Figure 5. Distributions of the host galaxies of those SBBH mergers as a function of galaxy stellar mass for different types of host galaxies, including central galaxies, satellites, and isolated galaxies.

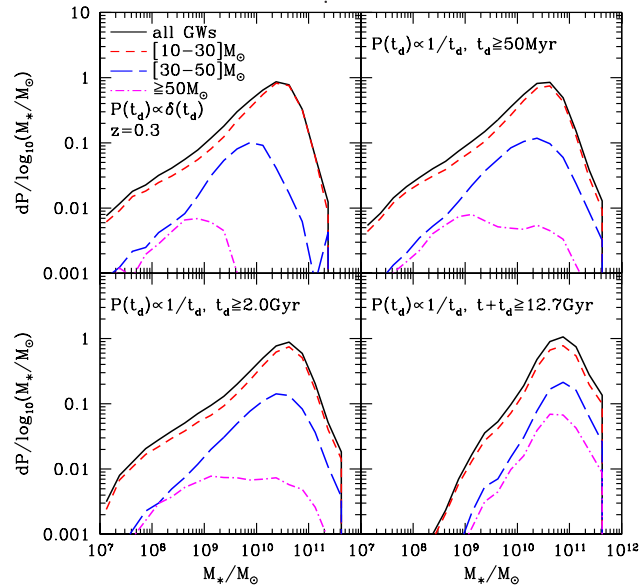


Figure 6. Stellar mass distributions of the host galaxies for SBBH mergers (at $z = 0.3$) with different total masses.

4.3 Host galaxies of SBBH mergers with different total masses

SBBHs with different total masses [$M_{\bullet\bullet} = M_{\bullet,1} + M_{\bullet,2} = (1+q)M_{\bullet,1}$] may have different formation histories. Heavy SBBHs may be formed only from metal poor binaries and thus in metal poor galaxies at early times, therefore, they should be hosted in galaxies with different properties from those lighter SBBHs at the SBBH merger time.

Figure 6 shows the stellar mass distributions of the host galaxies of SBBH GW events with different $M_{\bullet\bullet}$ at $z=0.3$. For the prompt model, the host galaxies of those

SBBH GW events with $M_{\bullet\bullet} \geq 50M_{\odot}$, similar to GW150914, GW170104, and GW170814, are small, with masses in the range from a few times 10^7M_{\odot} to a few times 10^9M_{\odot} (the magenta line in top-left panel of Fig. 6); while those for SBBH GW events with $M_{\bullet\bullet} \sim 30-50M_{\odot}$ and $\sim 10-30M_{\odot}$ peak at $6.7 \times 10^9M_{\odot}$ and $\sim 2.4 \times 10^{10}M_{\odot}$ with a 5 to 95 percentile stellar mass range of 3.8×10^8 to $2.7 \times 10^{10}M_{\odot}$ and 6.0×10^8 to $6.0 \times 10^{10}M_{\odot}$, respectively (blue long-dashed and red short-dashed lines). If those SBBH GW events formed at early time (e.g., $z \geq 6$ as the early SBBH formation model, bottom-right panel), then the host stellar mass distribution of those SBBH GW events with $M_{\bullet\bullet} \sim 30-50M_{\odot}$ (or $\sim 10-30M_{\odot}$) peaks at $9.4 \times 10^{10}M_{\odot}$ (or $7.5 \times 10^{10}M_{\odot}$) with a 5 to 95 percentile range of 9.4×10^9 to $2.4 \times 10^{11}M_{\odot}$ (or 6.7×10^9 to $2.1 \times 10^{11}M_{\odot}$); while those heavy SBBHs with $M_{\bullet\bullet} \geq 50M_{\odot}$, similar to GW150914 and GW170104, are hosted in galaxies that have stellar masses around $4.7 \times 10^{10}M_{\odot}$ with a 5 to 95 percentile range of 6.0×10^9 to $2.4 \times 10^{11}M_{\odot}$, similar to those for the host galaxies of lighter SBBHs ($10-50M_{\odot}$).

For other two $P_t(t_d)$ models with $t_d \geq 50$ Myr or ≥ 2 Gyr, i.e., the reference model and the large time delay model, the host galaxy stellar mass distribution of SBBHs with different $M_{\bullet\bullet}$ range are in between those resulting from the prompt model and the early SBBH formation model (with formation time $z > 6$). For those heavy SBBHs with $M_{\bullet\bullet} \geq 50M_{\odot}$, the host stellar mass distribution are broad and bimodal with one peak at $\sim 10^9M_{\odot}$ and the other peak at $\sim 2 \times 10^{10}M_{\odot}$, which are corresponding to a population formed recently in small galaxies and another population formed at early time in small galaxies but merged into big galaxies later.

4.4 Host galaxy metallicities

Since the formation of BHs depends on the metallicity of their progenitor stars, the formation of SBBHs is also dependent on the metallicity of their progenitor binary stars and thus the metallicity of the progenitor galaxies when they formed in. However, the metallicity of the host galaxies at the GW detection time may be significantly different from that of the progenitor galaxies at the SBBH formation time.

Figure 7 shows the host galaxy metallicity distributions of those SBBHs at their merger time (i.e., $z = 0.3, 1.0$, and 2.0 , respectively; thick lines in panels from top to bottom) and at formation time (thin lines), respectively. For those SBBH mergers at $z = 0.3$ produced from the reference model and the large time delay model, the host galaxy metallicity distributions at the SBBH formation time peak at $0.61Z_{\odot}$ and $0.53Z_{\odot}$, respectively. As expected, the larger the minimum time delay, the poorer the metallicity of the host galaxies at the SBBH formation time. The host galaxy metallicity distributions at the SBBH merger time resulting from these two models shift to higher metallicities due to the metal enrichment after the SBBH formation, and the difference between the two distributions are relatively small.

If those SBBHs were formed at early time, e.g., $z \geq 6$ (the early SBBH formation model), then they were mostly formed in metal poor small galaxies with metallicity peaking at $0.26Z_{\odot}$ and almost half of them having $Z \lesssim 0.12$ (thin dot-dashed magenta line). However, their host galaxies at the SBBH merger time ($z = 0.3$) have metallicities around $Z \sim$

0.57 Z_{\odot} with a 5 to 95 percentile range of 0.41 to 0.84 Z_{\odot} . In this case, even if the SBBH mergers were detected at high redshifts (e.g., $z = 1$ or 2), their host galaxies are still quite metal rich ($Z \sim 0.39 - 0.73Z_{\odot}, 0.30 - 0.65Z_{\odot}$ for $z = 1$ or 2 respectively), and have metallicities on average only slightly lower than those detected at lower redshift (e.g., $z = 0.3$).

To further illustrate the difference between the metallicities of the host galaxies at the SBBH formation time and that at the SBBH merger time, in Figure 8 we plot those mock SBBH mergers at $z = 0.3$ obtained from the reference model (red filled circles) and the early SBBH formation model (open blue circles) on the plane of the host galaxy metallicities at the SBBH merger time (Z_{obs}/Z_{\odot}) versus those at the SBBH formation time ($Z_{\text{ZAMS}}/Z_{\odot}$). This figure clearly shows that the metallicities of most SBBH host galaxies are enriched significantly after the formation of SBBHs, and the longer the time delay of the SBBH mergers, the more significant metal enrichment of the SBBH host galaxies.

According to Figures 7 and 8, the host galaxy metallicity distribution of those SBBH mergers that were formed at an early cosmic time in relatively metal poor galaxies is significantly less extended at the low metallicity end than that for those SBBHs formed at a later cosmic time in both metal rich and poor galaxies. This seemingly surprise result is caused by that most of those extremely metal poor host galaxies of SBBHs formed at early cosmic time are significantly metal enriched by star formation later.

Figure 9 shows the metallicity distributions of the host galaxies for SBBHs with different total mass ($M_{\bullet\bullet}$) range (i.e., 10–30 M_{\odot} , 30–50 M_{\odot} , and $\geq 50M_{\odot}$) at both the SBBH formation time and the SBBH merger time. For SBBH mergers with $M_{\bullet\bullet} \geq 50M_{\odot}$, they must be formed in galaxies with metallicities $\lesssim 0.2 - 0.3Z_{\odot}$ whenever their GW signals were detected at low redshift (e.g., $z = 0.3$) or high redshift (e.g., $z = 2$) and whenever the time delays is longer or shorter, which is primarily due to that the heavy SBBHs can only be formed from metal poor binary stars. However, the metallicities of their host galaxies at the SBBH merger time are all substantially metal richer with a 5 to 95 percentile range of 0.41 to 0.84 Z_{\odot} and have a distribution skewed toward high metallicities if those SBBHs were formed at $z \geq 6$, or they have a 5 to 95 percentile range of 0.07 to 0.65 Z_{\odot} (or 0.08 to 0.65 Z_{\odot}) and a distribution extending to low metallicities ($Z < 0.1Z_{\odot}$) if those SBBHs were formed at a time 50 Myr (or 2 Gyr) before the detection of their GW signals, or are also metal poor, i.e., $\lesssim 0.2 - 0.3Z_{\odot}$ if they merger shortly after their formation.

For light SBBHs, e.g., $M_{\bullet\bullet} = 10 - 30M_{\odot}$, they can be formed in galaxies with a large metallicity range (e.g., Z extends to 1.1 Z_{\odot}) whenever their GW signals are detected at low redshift or high redshift and whenever the time delay is longer or shorter. At the SBBH merger time, their host metallicities distribute over an even larger range with broader extensions at both the high Z and the low Z ends compared with that for $M_{\bullet\bullet} \geq 50M_{\odot}$. For SBBHs with intermediate mass [$M_{\bullet\bullet} \in (30 - 50M_{\odot})$], the distributions of the host metallicities at both the SBBH formation time and the SBBH merger time are in between those for the heavy SBBHs and for the light SBBHs (see Figure 9).

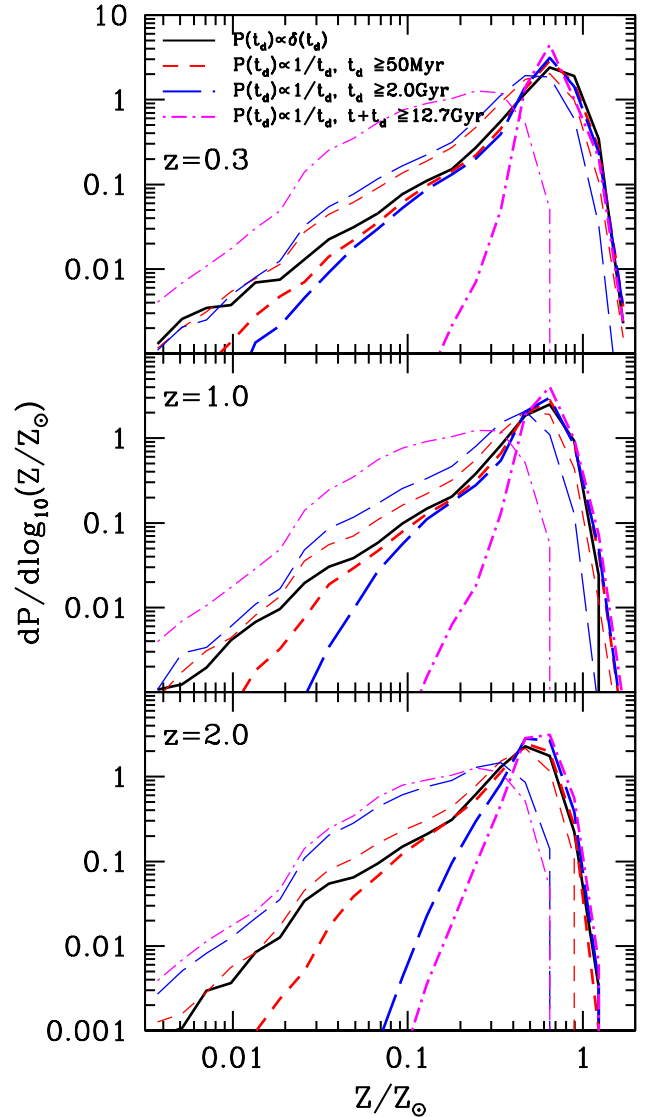


Figure 7. Metallicity distribution of the host galaxies at the SBBH formation time (thin lines) and the GW detection time or the SBBH merger time (thick lines). Legends for the lines and models are similar to Fig. 2.

5 CONCLUSIONS AND DISCUSSIONS

In this paper, we investigate the host galaxies of SBBH mergers, i.e., gravitational wave sources that may be detected by aLIGO and advanced VIRGO (VIRGO), by implementing simple SBBH formation recipes into cosmological galaxy formation model using the Millennium-II simulation with a large box of side 137 Mpc, and we present a complete and thorough analysis of the properties of the SBBH host galaxy. Our main results are summarized as follows.

SBBH mergers with total mass $M_{\bullet\bullet} \geq 10M_{\odot}$ at low redshift ($z \lesssim 0.3$) occur preferentially in massive galaxies with stellar mass $\gtrsim 2 \times 10^{10}M_{\odot}$ if the delay time between the SBBH formation and the merger is distributed in a broad range from less than Gyr to the Hubble time, and they occur preferentially in even more massive galaxies ($\sim 8 \times 10^{10}M_{\odot}$) if they were mostly formed at high redshift, e.g., $z > 6$ and

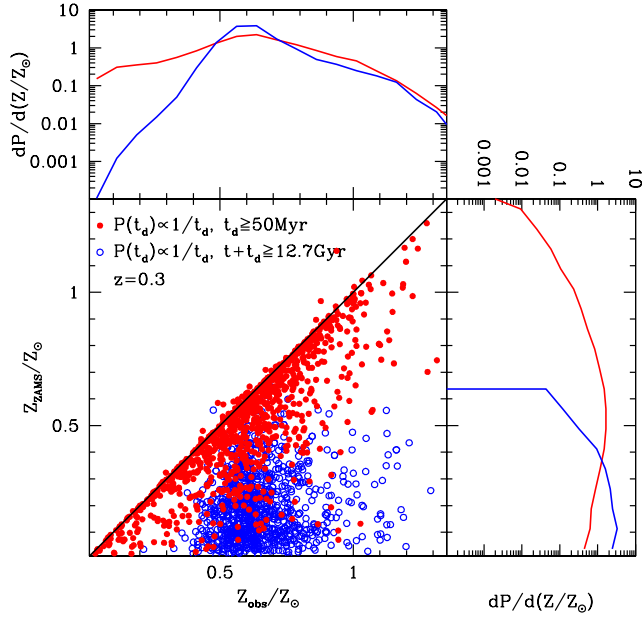


Figure 8. Randomly selected mock SBBHs on the plane of the metallicity of the host galaxy at the SBBH formation time versus the metallicity of the host galaxy at SBBH merger time. Red filled circles and blue open circles represent those mock SBBHs obtained from the early SBBH formation model and the reference model, i.e., $P(t_d) \propto 1/t_d$ with $t_d \geq 50$ Myr, and $t_d \geq 12.7$ Gyr – $t(z)$, respectively.

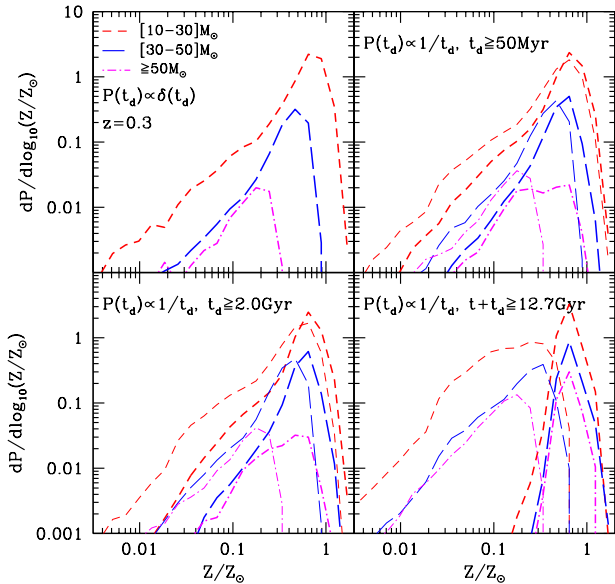


Figure 9. Metallicity distribution of those SBBH mergers with different mass ranges at both the SBBH detection time ($z = 0.3$; thick lines) and the SBBH formation time (thin lines). The red short dashed, blue long-dashed, and magenta dot-dashed lines in each panel represent the host galaxy metallicity distribution for mock SBBHs with total mass $M_{\bullet\bullet} = 10 - 30 M_{\odot}$, $30 - 50 M_{\odot}$, and $\geq 50 M_{\odot}$, respectively. Panels from top to bottom, left to right, show the results obtained from the prompt model, the reference model, the large time delay model, and the early SBBH formation model, respectively.

have a large delay time ($\gtrsim 13$ Gyr). For those heavy SBBH mergers ($M_{\bullet\bullet} \geq 50 M_{\odot}$), similar to GW 150914, GW 170104, and GW170814, their host stellar mass distribution is probably bimodal, with a low mass peak of $\sim 10^9 M_{\odot}$ and a high mass peak of $\sim 2 \times 10^{10} M_{\odot}$, if the delay time is distributed in a broad range from less than Gyr to the Hubble time. The lower peak is mainly contributed by those SBBHs formed recently ($z \lesssim 0.5$), while the higher mass peak is mainly contributed by those SBBHs formed at early time ($z \gtrsim 3.0$). If those heavy SBBH mergers detected at low redshift (e.g., $z \lesssim 0.3$) were formed only at early time (e.g., $z > 6$) or from Pop III stars, then their host galaxies were originally small at the SBBH formation time but became very massive (mainly $\gtrsim 3 \times 10^{10} M_{\odot}$) at the GW detection time because of later assembly and growth, and the fraction of the host galaxies with mass $\lesssim 10^9 M_{\odot}$ is negligible ($\lesssim 1\%$).

Some of these findings have been reported recently in Lamberts et al. (2016), Elbert et al. (2017), O’Shaughnessy et al. (2017), and Schneider et al. (2017). For example, Lamberts et al. (2016) found that GW 150914-like heavy SBBHs are likely to be found in massive galaxies, but at a significant fraction of such mergers should be hosted in dwarf galaxies formed at low redshift ($z \sim 0.5$), roughly consistent with our results for heavy SBBH mergers resulting from the reference model. Similar results may be also inferred from Elbert et al. (2017) as they stated that GW events would be preferentially localized in dwarf galaxies if the merger timescale is short compared to the age of the universe and in massive galaxies otherwise. O’Shaughnessy et al. (2017) and Schneider et al. (2017) also found that most GW 150914-like SBBH mergers should be hosted in star forming massive galaxies with stellar mass $\gtrsim 10^{10} M_{\odot}$ by implementing binary population synthesis models into simulations of either several galaxies or a small box. In addition, Schneider et al. (2017) also showed that fraction of GW 150914 like events in low mass galaxies decreases, but it is not zero. As the GW 150914-like candidates produced in Schneider et al. (2017) all have very long delay time, their host galaxy distribution is more or less like the one shown by the magenta line in the bottom right panel of Figure 6. Some of the quantitative differences of our results from those other studies may be due to the different settings for the SBBH formation model. Further studies by utilizing large volume simulations, such as Illustris (Vogelsberger et al. 2014) and EAGLE (Schaye et al. 2015) with a large variety of mock galaxies, and implementation of binary population synthesis would be necessary to accurately predict the properties (including stellar mass and metallicity) of the host galaxies of SBBH mergers and achieve better statistics.

We find that the host galaxies of GWs events detected at a high redshift also have a broad mass distribution. The host galaxy mass distributions at high redshifts obtained from different delay time models have similar trends as those obtained at low redshift (e.g., $z = 0.3$), and their peaks shift toward lower masses and the fraction of host galaxies at the low (or high) mass end increases (or decreases) with increasing GW detection redshift.

We find that the host galaxies of SBBH mergers with $M_{\bullet\bullet} \geq 10 M_{\odot}$ at low redshift (e.g., $z \lesssim 0.3$) are mostly spiral galaxies with stellar mass $\sim 5.3 \times 10^8 - 6.0 \times 10^{10} M_{\odot}$ and only \sim ten percent are in elliptical galaxies if the time period

between the SBBH formation and merger is distributed in a broad range from \lesssim Gyr to the Hubble time. However, about half of the hosts of those SBBH mergers detected by GW at low redshift (e.g., $z \lesssim 0.3$) should be elliptical galaxies if those SBBHs were formed at early time or from Pop III stars (e.g., $z \gtrsim 6$). The fraction of SBBH GW events that are hosted in elliptical galaxies depends on when those SBBHs were formed and merged, and it increases with the increasing of the time delay between SBBH formation and merger. We also find that most of the host galaxies of SBBH mergers detected by GW at low redshift should be central galaxies and only about 20% of them are satellite galaxies, which is almost independent of the settings of the delay time.

The formation of SBBHs depends on the metallicity of their progenitor binary stars. Heavy SBBHs ($M_{\bullet\bullet} \geq 50M_{\odot}$) were mostly formed in metal poor small galaxies with metallicities $\lesssim 0.2 - 0.3Z_{\odot}$. If the time delay between SBBH formation and merger covers a range from less than Gyr to the Hubble time, the host galaxy metallicity distribution of SBBH mergers (with total mass $M_{\bullet\bullet} \geq 10M_{\odot}$) detected at redshift $z \lesssim 0.3$ peaks around $0.6Z_{\odot}$ and has a long skewed wing towards the low metallicity end ($Z < 0.2Z_{\odot}$). The host galaxy metallicity distribution of heavy SBBHs (with total mass $\gtrsim 50M_{\odot}$, similar to GW 150914, GW 170104, and GW170814) at the merger time at redshift $z \lesssim 0.3$ is ranging from $Z < 0.1Z_{\odot}$ to $\sim 1.0Z_{\odot}$, substantially broader compared with that for less heavy SBBHs, and the fraction of host galaxies of the heavy SBBHs with $Z \lesssim 0.2Z_{\odot}$ is much larger than that for less heavy SBBHs. If SBBHs were formed at early time (e.g., $z > 6$; or from Pop III stars), their mergers detected at $z \lesssim 0.3$ occur preferentially in galaxies mostly with metallicities $\gtrsim 0.2Z_{\odot}$ and peaking around $Z \sim 0.6Z_{\odot}$, because of significant metal enrichment of those host galaxies after the SBBH formation. It is interesting to note here that the host galaxy metallicity distribution for the mergers of those heavy SBBHs that were initially formed at an early cosmic time (e.g., $z > 6$) in metal poor galaxies, is significantly less extended at the low metallicity end than that for those mergers of SBBHs formed at a later cosmic time in both metal rich and poor galaxies. This is seemingly a surprise result, as heavy SBBHs have to be formed in more metal poor galaxies.

Searching for the EM counterparts of SBBH GW sources is important for understanding the origin of those SBBHs and the application of them as probes to cosmology. However, currently it is still difficult to find these EM counterparts, if any, since the localization of these sources by GW signals is poor. If the properties of the host galaxies of SBBH mergers can be well understood as the efforts made in this study and others (e.g., Lamberts et al. 2016; O’Shaughnessy et al. 2017; Elbert et al. 2017; Schneider et al. 2017), the search for EM counterparts will be greatly narrowed and the host galaxies of SBBHs may be statistically determined even without EM counterpart information. Furthermore, if future observations can discover the EM counterparts and host galaxies of those SBBH mergers that will be detected by aLIGO, VIRGO, and other future GW observatories, and thus may provide important data to constrain the SBBH formation model and reveal the origin of those SBBHs.

ACKNOWLEDGEMENTS

This work is partly supported by the National Natural Science Foundation of China under grant No. 11690024, 11373031 and 11390372, the Strategic Priority Program of the Chinese Academy of Sciences (Grant No. XDB 23040100), and the National Key Program for Science and Technology Research and Development (Grant No. 2016YFA0400704).

REFERENCES

- Abbott, B. P., Abbott, R., Abbott, T. D., et al. 2016, *Physical Review Letters*, 116, 061102
- Abbott, B. P., Abbott, R., Abbott, T. D., et al. 2016, *Physical Review Letters*, 116, 241103
- Abbott, B. P., Abbott, R., Abbott, T. D., et al. 2016, *Living Reviews in Relativity*, 19, 1
- Abbott, B. P., Abbott, R., Abbott, T. D., et al. 2016, *ApJ*, 826, L13
- Abbott, B. P., Abbott, R., Abbott, T. D., et al. 2016, *ApJ*, 818, L22
- Abbott, B. P., Abbott, R., Abbott, T. D., et al. 2016, *Physical Review Letters*, 116, 131102
- Abbott, B. P., Abbott, R., Abbott, T. D., et al. 2017, *Physical Review Letters*, 118, 221101
- Abbott, R., et al. 2017, arXiv:1709.09660
- Abbott, B. P., Abbott, R., Abbott, T. D., et al. 2017, *Physical Review Letters*, 119, 161101
- Abbott, B. P., Abbott, R., Abbott, T. D., et al. 2017, *ApJ*, 848, L13
- Belczynski, K., Kalogera, V., & Bulik, T. 2002, *ApJ*, 572, 407
- Belczynski, K., Kalogera, V., Rasio, F. A., et al. 2008, *ApJS*, 174, 223-260
- Belczynski, K., Repetto, S., Holz, D. E., et al. 2016a, *ApJ*, 819, 108
- Belczynski, K., Holz, D. E., Bulik, T., & O’Shaughnessy, R. 2016b, *Nature*, 534, 512
- Boylan-Kolchin, M., Springel, V., White, S. D. M., Jenkins, A., & Lemson, G. 2009, *MNRAS*, 398, 1150
- Breivik, K., Rodriguez, C. L., Larson, S. L., Kalogera, V., & Rasio, F. A. 2016, arXiv:1606.09558
- Chabrier, G. 2003, *PASP*, 115, 763
- de Mink, S. E., Langer, N., Izzard, R. G., Sana, H., & de Koter, A. 2013, *ApJ*, 764, 166
- Dominik, M., Belczynski, K., Fryer, C., et al. 2013, *ApJ*, 779, 72
- Dvorkin, I., Vangioni, E., Silk, J., Uzan, J.-P., & Olive, K. A. 2016, *MNRAS*, 461, 3877
- Dvorkin, I., Uzan, J.-P., Vangioni, E., & Silk, J. 2017, arXiv:1709.09197
- Elbert, O. D., Bullock, J. S., & Kaplinghat, M. 2017, arXiv:1703.02551
- Farr, W. M., Sravan, N., Cantrell, A., et al. 2011, *ApJ*, 741, 103
- Fryer, C. L., Belczynski, K., Wiktorowicz, G., et al. 2012, *ApJ*, 749, 91
- Hartwig, T., Volonteri, M., Bromm, V., et al. 2016, *MNRAS*, 460, L74
- Hurley, J. R., Pols, O. R., & Tout, C. A. 2000, *MNRAS*, 315, 543
- Hurley, J. R., Tout, C. A., & Pols, O. R. 2002, *MNRAS*, 329, 897
- Guo, Q., White, S., Boylan-Kolchin, M., et al. 2011, *MNRAS*, 413, 101
- Lamberts, A., Garrison-Kimmel, S., Clausen, D. R., & Hopkins, P. F. 2016, *MNRAS*, 463, L31
- Madau, P., & Dickinson, M. 2014, *ARA&A*, 52, 415M
- Mandel, I. 2016, *MNRAS*, 456, 578
- Mandel, I., & de Mink, S. E. 2016, *MNRAS*, 458, 2634

- Mapelli, M. 2016, MNRAS, 459, 3432
- Mapelli, M., Giacobbo, N., Ripamonti, E., & Spera, M. 2017, arXiv:1708.05722
- McKernan, B., Ford, K. E. S., Bellovary, J., et al. 2017, arXiv:1702.07818
- Mirabel, I. F. 2016, arXiv:1609.08411
- Nakazato, K., Niino, Y., & Sago, N. 2016, arXiv:1605.02146
- Nakamura, T., Ando, M., Kinugawa, T., et al. 2016, Progress of Theoretical and Experimental Physics, 2016, 093E01
- Oguri, M. 2016, Phys. Rev. D, 93, 083511
- O'Shaughnessy, R., Kim, C., Kalogera, V., & Belczynski, K. 2008, ApJ, 672, 479-488
- O'Shaughnessy, R., Kalogera, V., & Belczynski, K. 2010, ApJ, 716, 615
- O'Shaughnessy, R., Bellovary, J. M., Brooks, A., et al. 2017, MNRAS, 464, 2831
- Özel, F., Psaltis, D., Narayan, R., & McClintock, J. E. 2010, ApJ, 725, 1918
- Perna, R., Chruslinska, M., Corsi, A., & Belczynski, K. 2017, arXiv:1708.09402
- Portegies Zwart, S. F., & Verbunt, F. 1996, A&A, 309, 179
- Raccanelli, A., Kovetz, E. D., Bird, S., Cholis, I., & Muñoz, J. B. 2016, Phys. Rev. D, 94, 023516
- Repetto, S., Davies, M. B., & Sigurdsson, S. 2012, MNRAS, 425, 2799
- Rodriguez, C. L., Morscher, M., Pattabiraman, B., et al. 2015, Physical Review Letters, 115, 051101
- Rodriguez, C. L., Chatterjee, S., & Rasio, F. A. 2016, Phys. Rev. D, 93, 084029
- Sasaki, M., Suyama, T., Tanaka, T., & Yokoyama, S. 2016, Physical Review Letters, 117, 061101
- Schaye, J., Crain, R. A., Bower, R. G., et al. 2015, MNRAS, 446, 521
- Schneider, R., Graziani, L., Marassi, S., et al. 2017, arXiv:1705.06781
- Spera, M., Mapelli, M., & Bressan, A. 2015, MNRAS, 451, 4086
- Spera, M., & Mapelli, M. 2017, MNRAS, 470, 4739
- Springel, V., White, S. D. M., Jenkins, A., et al. 2005, Nature, 435, 629
- Strolger, L.-G., Riess, A. G., Dahlen, T., et al. 2004, ApJ, 613, 200
- Vogelsberger, M., Genel, S., Springel, V., et al. 2014, MNRAS, 444, 1518
- Wang, L., Spurzem, R., Aarseth, S., et al. 2016, MNRAS, 458, 1450
- Wang, S., Wang, Y.-F., Huang, Q.-G., & Li, T. G. F. 2016, arXiv:1610.08725
- Woosley, S. E., & Weaver, T. A. 1995, ApJS, 101, 181

This paper has been typeset from a $\text{\TeX}/\text{\LaTeX}$ file prepared by the author.